Available online at www.sciencedirect.com
SCIENCE DIRECT®
Composite Structures 67 (2005) 427–436
COMPOSITE STRUCTURES
www.elsevier.com/locate/compstruct

A micromechanics approach for damage modeling of polymer matrix composites

E.J. Barbero [a,*], G.F. Abdelal [b], A. Caceres [c]

[a] Mechanical and Aerospace Engineering, 315 Engineering Science Building, West Virginia University, Morgantown, WV 26505, USA
[b] National Authority for Remote Sensing and Space Science, Giza, Egypt
[c] Department of Civil Engineering, University of Puerto Rico at Mayagüez, Mayagüez, PR 00681-9041, Puerto Rico

Available online 25 March 2004

Abstract

A new model for damage evolution in polymer matrix composites is presented. The model is based on a combination of two constituent-level models and an interphase model. This approach reduces the number of empirical parameters since the two constituent-level models are formulated for isotropic materials, namely fiber and matrix. Decomposition of the state variables down to the micro-scale is accomplished by micromechanics. Phenomenological damage evolution models are then postulated for each constituent. Determination of material parameters is made from available experimental data. The required experimental data can be obtained with standard tests. Comparison between model predictions and additional experimental data is presented.

Keywords: Damage mechanics; Micromechanics; Composites; Stress concentration; Strain concentration; Periodic microstructure

1. Introduction

Using classical laminate theory and other similar approaches, polymer matrix composites (PMC) are routinely analyzed by assembling laminae response into laminate response models [8]. The laminate-level response to external loads is then decomposed into laminae responses. That is, the point stress and strains on each homogeneous orthotropic lamina are found. When this approach is applied to modeling of damage, the major shortcoming is the large number of material constants required to represent the equivalent orthotropic material [4–6,22]. There are only few material systems for which the whole set of stiffness and strength values are available from experimental data. Each new fiber/matrix combination requires a lengthy and expensive material characterization effort. The data are scarcer with regards to damage evolution.

Advances in micromechanics allow us to predict lamina-scale stiffness from constituent (fiber, matrix) properties. Some micromechanical models [15,23] make it possible to decompose the lamina-scale state variables (e.g., stress, strain, damage) into their components in each of the constituents. Therefore, damage evolution models and failure criteria can be formulated at the constituent-level. The model proposed herein accounts for different initiation, evolution, and failure of the two main constituents (fiber and matrix) and, with the addition of an interphase model, it accounts for other effects not captured by the constituent models. Loss of transverse isotropy at the lamina-level due to damage can be predicted [12]. The material parameters are determined by modeling standard material tests and adjusting individual material parameters to reproduce the observed material response. Then, model predictions for independent test conditions are compared with their corresponding test data.

In laminate analysis, each lamina is considered as a homogeneous material. The characteristic length of a material element over which the stress and strains do not change rapidly is the lamina thickness. The fiber diameter, fiber spacing, and dimensions of micro-cracks are much smaller than the lamina thickness. Therefore, fiber breaks, matrix crazes and micro-cracks can be analyzed as distributed damage. Since damage of the fiber phase contributes only to loss of stiffness and strength in the fiber direction, the characteristic length of the fiber phase is of the order of the fiber length, supporting the

* Corresponding author. Fax: +1-304-2936689.
E-mail address: ebarbero@wvu.edu (E.J. Barbero).

0263-8223/$ - see front matter © 2004 Elsevier Ltd. All rights reserved.
doi:10.1016/j.compstruct.2004.02.001

assumption that fiber breaks can be modeled as distributed damage [19,29]. In tensile loading normal to the fibers, matrix cracks grow along the fiber length and can exceed the lamina thickness, which seems to invalidate the assumption of distributed damage. But if that happens to a unidirectional lamina, such cracks lead to immediate failure. However, if such cracks grow in a laminate, their growth is controlled by the adjacent laminae and thus can be thought of distributed damage in the context of the laminate, not the lamina where they occur. In other words, transverse cracks can be still be accounted for by a CDM model in a lamina provided such lamina is part of a laminate, which is the practical case virtually all the time. An alternative option would be to formulate the damage model completely at the lamina level [4,5,21]. Such approach requires a more extensive database of lamina strength values. In this work, it was decided to use the constituent-level approach because of the basic nature of the strength data required, namely fiber strength, Weibull dispersion, and so on.

2. Damage model

The overall damage model is based on the combination of damage models for fiber, matrix, and interphase [2,32–35]. All three damage models are based on the concepts of continuous damage mechanics [20]. For each phase, damage is represented by a state variable, in the form of a second-order damage tensor D_{ij}, or by its complement the integrity tensor $\Omega_{ij} = \delta_{ij} - D_{ij}$. To preserve the symmetry of the effective stress tensor, a fourth-order damage-effect tensor is used to compute the effective stress from the damaged one. The damage-effect tensor **M** is univocally determined in terms of the second-order damage tensor **D**. Since tension, compression, and shear have different effects on damage, crack closure coefficients ($0 < c_n < 1$ and $0 < c_s < 1$), for compression and shear, respectively, are introduced in the definition of the damage-effect tensor, as follows

$$\begin{aligned}\overline{\sigma}_{ij} &= M_{ijkl}\sigma_{kl}\\ M_{ijkl} &= \frac{\zeta_{ijkl}\langle\sigma_{kl}\rangle}{1-D_{ij}} + \frac{\zeta_{ijkl}\langle-\sigma_{kl}\rangle}{1-c_nD_{ij}}\\ &\quad + \frac{I_{ijkl}-\zeta_{ijkl}}{2}\left[\frac{1}{1-c_sD_{ii}} + \frac{1}{1-c_sD_{ii}}\right]\end{aligned} \tag{1}$$

where $\zeta_{ijkl} = 1$ if $i = j = k = l = 1$, zero otherwise, and $\langle\rangle$ is the McAuley bracket.

The analysis uses three configurations: effective ($\overline{\sigma}$), partially damaged ($\tilde{\sigma}$) and damaged (σ). In the effective configuration, the undamaged portion of fiber and matrix carry the load. In the partially damaged configuration, the fiber and matrix have distributed damage but the interphase damage is not present. In the damaged configuration, all the damage is present. The three configurations are illustrated in Fig. 1, starting with *damaged* on the right, *partially damaged* at the center, and *effective* on the left. These configurations are similar to those proposed in [32–35]. The model is phenomenological and damage is assumed to be distributed. Therefore, the model cannot predict microscopic features such as crack spacing [16,25,27,28,30]. All forms of damage are homogenized and their effect is felt on the reduced stiffness only.

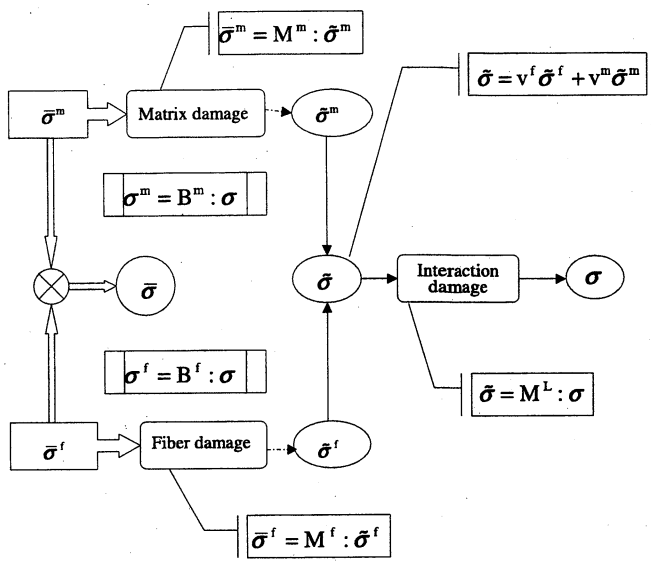

Fig. 1. Damage configurations, from left to right, effective, partially damaged, and damaged.

Mapping between configurations is accomplished by the appropriate damage effect tensor, M^L from damaged to partially damaged (due to interphase damage-effects), M^f and M^m from partially damaged to effective for fiber and matrix phases, respectively. The total damage-effect tensor **M** that accounts for the combined effect of fiber, matrix, and interphase damage is given by

$$M_{ijrs} = (c^f M^f_{ijkl}B^f_{kluv} + c^m M^m_{ijkl}B^m_{kluv})M^L_{uvrs} \tag{2}$$

At each configuration, mapping between phases (fiber, matrix, and interphase) is accomplished by micromechanics using the stress and strain concentration tensors, **B** and **A**, respectively, according to

$$\begin{aligned}\sigma^r &= B^r : \sigma;\ B^r = C^r : A^r : C^{-1}\\ \varepsilon^r &= A^r : \varepsilon;\ A^r = C^{-f} : B^r : C\end{aligned} \tag{3}$$

where σ^r indicates the stress in the phase $r = $ f, m, l, and σ is the stress in the homogenized material. In this work, these tensors represent the mapping of average stress and strains, which are averaged over the individual phases. The stiffness tensor **C** of one configuration (say damaged) is obtained in terms of the stiffness $\overline{C}$ of the precursor configuration (say virgin) by using the energy equivalence principle [20], as

$$C = M^{-1} : \overline{C} : M^{-1} \tag{4}$$

Eq. (3) account for the stress redistribution between the fiber and the matrix that must take place when both

phases undergo damage at different rates. Stress redistribution also takes place at the macro-level (among laminae) as a result of updating the lamina stiffness tensor **C** according to Eq. (4).

The stress and strain concentration tensors are obtained using [23] in the effective configuration. Then, the concentration tensors in the partially damaged configuration are computed as

$$\begin{aligned}\widetilde{A}^{\mathrm{f}} &= [v^{\mathrm{m}}M^{-m}\overline{A}^{\mathrm{m}}\overline{A}^{-f}M^{-f} + v^{\mathrm{f}}I]^{-1}\\ \widetilde{A}^{\mathrm{m}} &= \frac{1}{v^{\mathrm{m}}}[I - v^{\mathrm{f}}\widetilde{A}^{\mathrm{f}}]\\ I_{ijkl} &= \frac{1}{2}(\delta_{ik}\delta_{jl} + \delta_{il}\delta_{jk})\end{aligned} \tag{5}$$

Similar equations are used to compute the concentration tensors in the damaged configuration in terms of the same in the partially damaged one. Also for each configuration, the stiffness tensor of the homogenized material is computed by $C = v^{\mathrm{f}}C^{\mathrm{f}}A^{\mathrm{f}} + v^{\mathrm{m}}C^{\mathrm{m}}A^{\mathrm{m}}$, where v^{f} and v^{m} are the fiber and matrix volume fractions of the current configuration. The volume fractions in the damaged configuration are those determined during fabrication of the composite. The volume fractions in the effective configuration are different that those in the damaged configuration because the effective configuration deals with the volume of undamaged fiber and matrix, both of which are different from the original volumes of fiber and matrix of the as-produced composite. The fiber and matrix volume fractions in the effective configuration are computed by taking into account the amount of damaged volume in the fiber and matrix phases [2,11], as follows

$$\begin{aligned}\overline{v}^{r} &= \frac{v^{r}(1 - D^{r}_{\mathrm{eq}})}{v^{\mathrm{f}}(1 - D^{\mathrm{f}}_{\mathrm{eq}}) + v^{\mathrm{m}}(1 - D^{\mathrm{m}}_{\mathrm{eq}})}\\ D^{r}_{\mathrm{eq}} &= (D^{r}_{ij}D^{r}_{ij})^{1/2}\end{aligned} \tag{6}$$

3. Damage evolution

A damage surface is assumed to limit the space of thermodynamic forces Y for which no damage occurs, as follows

$$g(Y,\gamma) = \sqrt{Y : J : Y} + \sqrt{|H : Y|} - (\gamma + \gamma_0) \tag{7}$$

where **J** and **H** are second-order tensors of material coefficients which are univocally related to the material properties of each phase, γ is the hardening parameter in Y-space, and γ_0 is the damage threshold in Y-space. In this work, an off-centered surface is used [5] to account for different behavior in tension and compression of each phase. Two two-dimensional views of the g-surface are shown in Fig. 2. The second-order tensor **Y** contains the thermodynamic forces, dual to the damage tensor, in the thermodynamic sense as $Y = \frac{\partial \psi}{\partial D} = \frac{1}{2}\frac{\partial}{\partial D}[C : \varepsilon : \varepsilon]$, where the free energy ψ is given by the sum of the strain energy π plus the damage dissipation potential Γ, as $\psi = \pi(\varepsilon, D) + \Gamma(\delta)$, where δ is an intermediate variable such that $\mathrm{d}\delta = -\mu$ and μ is the damage multiplier, obtained by satisfying the consistency conditions $g = 0$ and $\mathrm{d}g = 0$. Based on experimental observations [26,36], it is possible to assume that the damage principal directions coincide with the principal material directions, in which case the damage and integrity tensors become diagonal. With this simplification, it is possible to derive explicit equations relating the thermodynamic forces to the stress components. For example, using contracted notation [8] and a state of plane stress we have

$$\begin{aligned}Y_1 &= \frac{1}{\Omega_1^2}\left(\frac{\overline{C_{11}}}{\Omega_1^4}\sigma_1^2 + \frac{\overline{C_{12}}}{\Omega_1^2\Omega_2^2}\sigma_1\sigma_2 + \frac{\overline{C_{66}}}{\Omega_1^2\Omega_2^2}\sigma_6^2\right)\\ Y_2 &= \frac{1}{\Omega_2^2}\left(\frac{\overline{C_{22}}}{\Omega_2^4}\sigma_2^2 + \frac{\overline{C_{12}}}{\Omega_1^2\Omega_2^2}\sigma_1\sigma_2 + \frac{\overline{C_{66}}}{\Omega_1^2\Omega_2^2}\sigma_6^2\right)\\ Y_3 &= 0\end{aligned} \tag{8}$$

Using these explicit equations, the damage surface can be written in stress space, and its shape is the same as that of the Tsai-Wu quadratic failure criterion, but its size is variable as controlled by the magnitudes of the damage threshold γ_0 and hardening parameter γ. In summary, Eq. (7) reduces to

$$g = f_{ij}\sigma_i\sigma_j + f_i\sigma_i - (\gamma + \gamma_0); \quad (i = 1,2,\ldots,6) \tag{9}$$

Eq. (9) coincides with the Tsai-Wu criterion when $\gamma + \gamma_0 = 1$. Since the Tsai-Wu criterion predicts lamina failure in terms of available strength data, it is possible to determine all the coefficients of the tensors ***J*** and ***H*** in

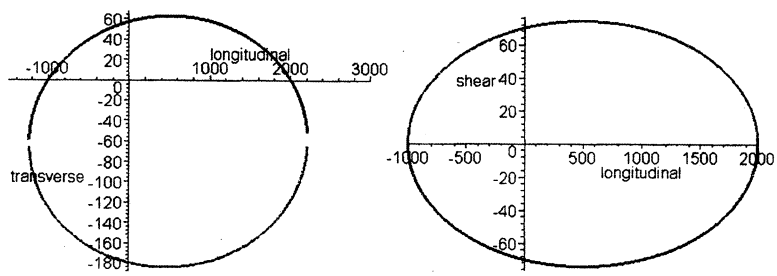

Fig. 2. Damage surface in thermodynamic force Y-space.

Table 1
Material properties for T300-5208

Property	Fiber	Matrix	Lamina
Modulus, E (GPa)	230	4.6	–
Poisson's ratio ν	0.22	0.38	0.284
Initial volume fraction	0.6	0.4	–
F_t, (GPa)	3.654	0.0586	1.550 (longitudinal)
F_c, (GPa)	1.096	0.1876	1.096 (longitudinal)
Critical D_t	0.105161	0.5	0.105161
Critical D_c	0.110945	0.5	0.110945
F_6, (GPa)	–	–	0.08616
G_{12}, (GPa)	104.545	1.667	5.090
Weibull dispersion m	0.89	–	–

Eq. (7), or f_{ij} and f_i in Eq. (9), in terms of available strength data for each phase (see Table 1), as described in Section 4. The size of the damage surface in Y-space evolves according to the following equation

$$\gamma(\mu) = \frac{\partial \psi}{\partial \delta} = c_1[1 + \exp(-\delta/c_2)]$$
$$d\delta = \mu \frac{\partial g}{\partial \gamma} = -\mu \tag{10}$$

in terms of two empirical parameters c_1 and c_2 to be determined from experiments. The damage multiplier μ is found interactively so that the consistency conditions $g = 0$ and $dg = 0$ are met. That is, after an increment of strain that causes damage, the Y-state must remain on the $g = 0$ surface with no further change of that surface ($dg = 0$). Once the damage surface is reached, damage accumulates along the normal to the damage-flow surface

$$f(Y,\gamma) = \sqrt{Y : J : Y} - (\gamma + \gamma_0) \tag{11}$$

The magnitude of additional damage is controlled by the damage multiplier so that (see Fig. 3) $dD_{ij} = \mu \frac{\partial f}{\partial Y_{ij}}$; $D_{ij} = \int dD_{ij}$; $\Omega_{ij} = \delta_{ij} - D_{ij}$. A transversely isotopic lamina may become orthotropic as a result of damage [12], which is allowed in the formulation by virtue of Eq. (4) using and orthotropic damage tensor **D** and damage-effect tensor **M**. Also, the model separates damage in the fiber and matrix, and redistributes the stress into the fiber and matrix.

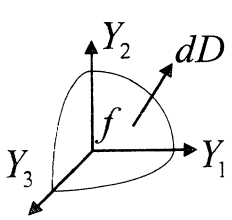

Fig. 3. Damage increment in thermodynamic force Y-space.

4. Determination of model parameters

Nine model parameters (three per phase) are necessary to track the evolution of damage. For each phase (fiber, matrix, and interphase), there are two parameters (c_1, c_2) in the evolution law Eq. (10) and the damage threshold γ_0 in Eq. (7). The nine parameters are determined by modeling standard material tests for which data are available. The procedure is illustrated using available data for T300/5208 (Table 1) [14] and LTM45EL-SM unidirectional tape data (Table 2) [38]. The intermediate parameters in Tables 3 and 4 are computed as explained in Section 5. The following procedure is used to adjust the nine damage parameters for each material.

First, a longitudinal tensile test (ASTM D3039 [3]) is simulated. The fiber parameters $(c_1^f, c_2^f, \gamma_0^f)$ are adjusted so that at failure the fiber stress equals the fiber strength F_{ft} and the fiber damage equals the known value $D_{ft} = 1 - \exp(-1/m)$, where m is the Weibull modulus [19,29], which is available [18,24,31] (Tables 1 and 2).

Second, a transverse tensile test is simulated [3]. The matrix parameters $(c_1^m, c_2^m, \gamma_0^m)$ are adjusted so that at failure the transverse stress equals the known transverse strength of the composite F_{mt} and the matrix damage equals $D_{mt} = 1/2$ as estimated by [17] (Tables 1 and 2).

Next, adjust the interphase parameters $(c_1^L, c_2^L, \gamma_0^L)$ to minimize any discrepancies between the shape of the shear stress-strain plot and the corresponding experimental data of a unidirectional lamina (see Section 5.3). This is illustrated in Figs. 4 and 5. The error is measured by the χ^2 statistical measure of the difference between the predicted values p_i and the experimental values e_i

$$\chi^2 = \frac{\sum(p_i^2 - e_i^2)}{\sum e_i^2} \tag{12}$$

The values obtained are shown in Tables 5 and 6. The model is then used to predict the response of other laminates. The predictions are then compared in Section 7 against experimental data that was not used to adjust the model parameters.

Table 2
Material properties for LTM45EL-SM

Property	Fiber	Matrix	Lamina
Modulus, E (GPa)	235	2.9	–
Poisson's ratio ν	0.2	0.38	0.3
Initial volume fraction	0.5	0.5	–
F_t, (GPa)	3.654	0.0281	1.330 (longitudinal)
F_c, (GPa)	1.173	0.0945	1.173 (longitudinal)
Critical D_t	0.105161	0.5	0.105161
Critical D_c	0.110945	0.5	0.110945
F_6, (GPa)	–	–	0.0745
G_{12}, (GPa)	96.311	0.760	4.0
Weibull dispersion m	0.89	–	–

Table 3
Intermediate coefficients in terms of properties in Table 1

Parameter	Fiber	Matrix	Interphase
H_1	0.263003×10^{-13}	0.214158×10^{-13}	0.147130×10^{-10}
$H_2 = H_3$	0.263003×10^{-13}	0.214158×10^{-13}	0.731900×10^{-13}
J_{11}	-0.142753×10^{-5}	-0.616990×10^{-6}	-0.313700×10^{-4}
$J_{22} = J_{33}$	-0.142753×10^{-5}	-0.616990×10^{-6}	0.129691×10^{-8}

Table 4
Intermediate coefficients in terms of properties in Table 2

Parameter	Fiber	Matrix	Interphase
H_1	−0.1947072329e−4	−0.7727031701e−6	−0.1056696052e−6
$H_2 = H_3$	−0.1947072329e−4	−0.7727031701e−6	0.4920883693e−2
J_{11}	0.2332145379e−12	0.1863544484e−13	0.3816379041e−15
$J_{22} = J_{33}$	0.2332145379e−12	0.1863544484e−13	0.9059230378e−8

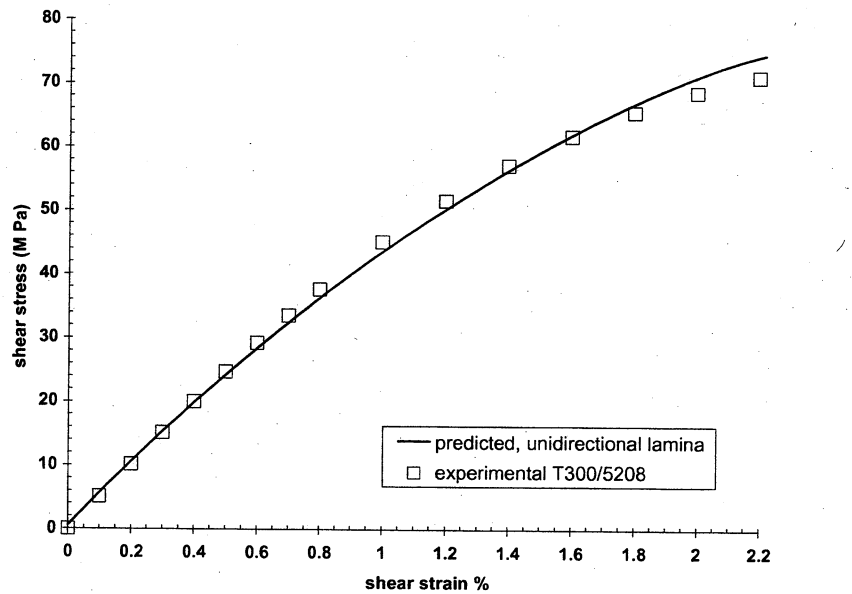

Fig. 4. Comparison of model prediction and experimental data for shear of T300/5208 unidirectional lamina.

5. Determination of intermediate constants

The coefficients in the second-order tensors **J** and **H** are intermediate constants introduced in order to write the damage surface in a concise form. They are not adjustable parameters. The values of the constants are determined univocally in terms of available stiffness and strength material properties. The relationship between the coefficients in **J** and **H** and the material properties is established in this section. Since the principal directions of damage in each phase is assumed to coincide with the material directions of the lamina, the tensors **J** and **H** are diagonal.

5.1. Intermediate constants for the matrix

Since the matrix is isotropic, $J_{33} = J_{22} = J_{11}$ and $H_{33} = H_{22} = H_{11}$. The values of J_{11} and H_{11} for the matrix are obtained by writing Eq. (7) for the case of tensile and compressive failure of the matrix as

$$\begin{aligned}\sqrt{J_{11}}\left(\frac{\overline{C}_{11}}{\Omega_t^6}\right)F_t^2+\sqrt{|H_{11}|\left(\frac{\overline{C}_{11}}{\Omega_t^6}\right)}&=1\\ \sqrt{J_{11}}\left(\frac{\overline{C}_{11}}{\Omega_c^6}\right)F_c^2+\sqrt{|H_{11}|\left(\frac{\overline{C}_{11}}{\Omega_c^6}\right)}&=1\end{aligned}\qquad(13)$$

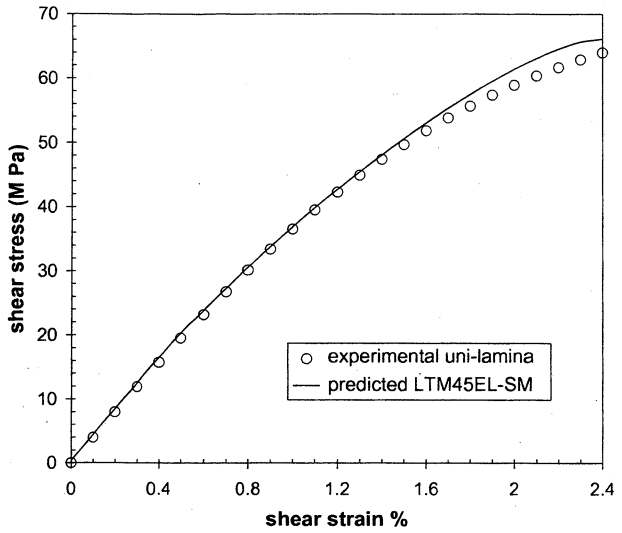

Fig. 5. Comparison of model prediction and experimental data for shear of LTM45EL-SM unidirectional lamina.

Table 5
Damage parameters for T300-5208

Parameter	Fiber	Matrix	Interphase
C_1	1.0	1.0	1.0
C_2	-1.1×10^5	-4.2×10^6	−1.5
γ_0	−6.5	2.0	0.0

Table 6
Damage parameters for LTM45EL-SM

Parameter	Fiber	Matrix	Interphase
c_1	1	1	1
c_2	−5e2	−6.2e6	−1.5
γ_0	−6.5	1.75	0

where $F_t = F_{mt}$, $F_c = F_{mc}$ are the tensile and compressive strength of the matrix, respectively, Ω_{mt} and Ω_{mc} are the critical values of integrity at failure. For a brittle matrix, $\Omega_{mt} = \Omega_{mc} = 0.5$ [17].

5.2. Intermediate constants for the fiber

Although anisotropic fibers are allowed by the model, it is more practical to assume that the fibers are isotropic. Then $J_{33} = J_{22} = J_{11}$ and $H_{33} = H_{22} = H_{11}$. The values of J_{11} and H_{11} for the fibers are obtained using Eq. (13) setting $F_t = F_{ft}$, $F_c = F_{fc}$ for the case of tensile and compressive failure of the fiber. In the case of fibers, the tensile strength of fiber F_{ft}, can be reached by subjecting a composite to longitudinal tensile loading but the compressive strength of fibers cannot be reached since the fibers buckle first. Therefore, F_{fc} corresponds to the compressive strength of the composite. The critical values of integrity for tensile behavior of the fibers is limited by the number of unbroken fibers at failure according to the weakest link model [19,29]; that is $\Omega_{ft} = \exp(-1/m)$ or about 0.894 for fiber Weibull dispersion $m = 8.9$ [18]. For compression, the critical integrity corresponds to the number of unbuckled fibers carrying load at the onset of kink-band formation, with can be approximated as

$$\Omega_{fc} = \operatorname{erf}\left(\frac{\alpha_{cr}}{\Gamma\sqrt{2}}\right) \tag{14}$$

where erf is the error function, α_{cr} is the fiber angle at failure, and Λ is the standard deviation of fiber misalignment [8–10,37]. Using data from the literature [7,13,14,21], Eq. (14) yields $\Omega_{fc} = 0.9$ for all the materials considered in this work.

5.3. Intermediate constants for the interphase

The effects of interphase damage are accounted for at the lamina level. Since a lamina is initially a transversely isotropic material, $J_{33} = J_{22}$ and $H_{33} = H_{22}$. The intermediate constants J_{11} and H_{11} can be found by considering the tensile and compressive tests of a unidirectional lamina. Therefore, using Eq. (13) with $F_t = F_{lt}$, $F_c = F_{lc}$ being the tensile and compressive strength of the lamina, respectively, Ω_t and Ω_c are the critical values of integrity at failure. For tensile behavior $\Omega_t = 0.1$ [19,29] and for compression $\Omega_c = 0.9$ [9]. The values of J_{22} and H_{22} are found as follows.

Let the fiber-reinforced lamina be subjected to a transverse uniaxial load, so that the only stress component different from zero is σ_2. The expression of the damage surface can be written in terms of the tensile failure strength of the material in the transverse direction. Then, the component J_{22} can be derived as a function of H_2 as

$$J_{22} = \left(1 - \sqrt{|H_2|\frac{\overline{C_{22}}}{\Omega_{2t}^6}F_{2t}}\right)^2 \left(\frac{\overline{C_{22}}}{\Omega_{2t}^6}F_{2t}\right)^{-2} \tag{15}$$

where the parameter Ω_{2t} is the critical value of the integrity component Ω_2 for tensile loading in the transverse direction. Since brittle fracture of the matrix controls the transverse tension strength of a lamina, the limiting value of the component Ω_2 of the integrity tensor can be found using the brittle loose bundle model [17], which yields $\Omega_{2t} = 0.5$.

Next, let us consider the fiber-reinforced lamina subject to a state of inplane shear, so that the only stress component different from zero is σ_6. In this case Eq. (6), in terms of the inplane shear strength of the lamina F_6, reduces to

$$\sqrt{\frac{J_{11}}{\Omega_{1s}^4}+\frac{J_{22}}{\Omega_{2s}^4}\frac{2\overline{C_{66}}}{\Omega_{1s}^2\Omega_{2s}^2}F_6^2}+\sqrt{\left|\frac{H_1}{\Omega_{1s}^2}+\frac{H_2}{\Omega_{2s}^2}\right|\frac{2\overline{C_{66}}}{\Omega_{1s}^2\Omega_{2s}^2}F_6}$$
$$=(\gamma^*+\gamma_0)=1 \tag{16}$$

where Ω_{1s} and Ω_{2s} are the critical values of the integrity component Ω_1, Ω_2 for a state of inplane shear stress. Since the shear response of a fiber-reinforced lamina along material principal directions is independent of the sign of the shear stress, the coefficient of the linear term in Eq. (16) must be zero, leading to the relationship

$$H_2=-\frac{\Omega_{2s}^2}{\Omega_{1s}^2}H_1=-r_sH_1;\quad r_s=\frac{\Omega_{2s}^2}{\Omega_{1s}^2} \tag{17}$$

Then, the component J_{22} can be written as a function of the parameter r_s using Eq. (15). Hence, Eq. (16) becomes

$$\sqrt{\frac{J_{11}r_s}{k_s}+\frac{J_{22}}{k_sr_s}\frac{2\overline{C_{66}}}{k_s}F_6^2}=1;\quad k_s=\Omega_{1s}^2\Omega_{2s}^2 \tag{18}$$

Finally, Eq. (18) can be solved to obtain the value of the parameter r_s, which is then used to compute J_{22} and H_2. Experimental evidence reveals a highly nonlinear behavior for a fiber-reinforced lamina subject to inplane shear. Writing the shear stress-strain law in the damaged and undamaged configurations we have

$$\overline{\sigma_6}=2\overline{G}_{12}\Omega_1\Omega_2\varepsilon_6=\frac{2G_{12}\varepsilon_6}{\Omega_1\Omega_2} \tag{19}$$

Calling G_{12}^* the value of the unloading (damaged) shear modulus just prior to failure, and $\overline{G}_{12}$ to the virgin shear modulus, we have

$$k_s=\Omega_{1s}^2\Omega_{2s}^2=G_{12}^*/\overline{G_{12}} \tag{20}$$

Thus, only the critical value of the product of the integrity parameters in shear can be determined and not their individual values. This is a consequence of the assumption that the principal directions of the second-order damage tensor **D** remain aligned with the material principal directions over the entire life of the material. Under these conditions, shear damage is interpreted as a combination of longitudinal and transverse matrix cracks, which is supported by experimental observations [26,36]. However, as experimentally observed, most of the damage is in the form of fiber-matrix debonding along the fibers, resulting in $D_{2s}>D_{1s}$, and from Eq. (17) we obtain a restriction on the value of r_s, namely $0<r_s<1$. Since all components of the damage tensor have values in the range zero to one, we obtain a restriction for the value of k_s, namely $0<k_s<1$. Such restrictions are useful while searching for the value of r_s, which is the root of Eq. (18). If the damaged shear modulus is know from experiments, the value of k_s can be determined univocally from Eq. (20). Otherwise, k_s can be taken as an additional adjustable parameter subject to the above mentioned restrictions.

6. Finite element implementation

The damage model was implemented as a user material subroutine (UMAT) into Abaqus [1]. The model updates the stress, damage, and stiffness at each Gauss point as a function of the increment of strain $\Delta\varepsilon$ provided by Abaqus. If $\Delta\varepsilon$ is too large, it is subdivided inside the UMAT to achieve convergence at the end of the De interval before returning to Abaqus.

Eight-node solid elements are used for the analysis. The layered structure inside the element is described in the standard Abaqus way [1]. Only *nine* empirical parameters are used to define the damage behavior of the material. These are c_1, c_2, and γ_0, for fiber, matrix, and interphase (Table 5). They are entered as parameters to the UMAT. The model, as implemented in the UMAT, calculates forty-two state variables internally. These are:

Nine components of the damage tensors; three for each phase.
Nine components of the thermodynamic force tensors, three for each phase.
Twelve components of the stress tensors, six for fiber and six for matrix.
Three values of the damage surface g for fiber, matrix, and interphase.
Three values of hardening γ for fiber, matrix, and interphase.
Three flags to indicate if the damage surface has been reached.

The problem is discretized in the usual way. Appropriate boundary conditions are applied on the discretization to simulate the strain field of the material tests used for validation.

7. Comparison with experimental data

The damage parameters for T300/5208 and LTM45EL-SM were determined in Section 4 using fiber and matrix properties, and a limited number of lamina properties. Several laminates are analyzed next by using the ABAQUS implementation of the damage model.

First, consider LTM45EL-SM, where SM stands for standard modulus fibers [38]. Comparison of predicted and experimental results for an inplane shear test of [0/90]s is shown in Fig. 6. Comparison of predicted and experimental results for an axial loading test of [45/–45]s is shown in Fig. 7.

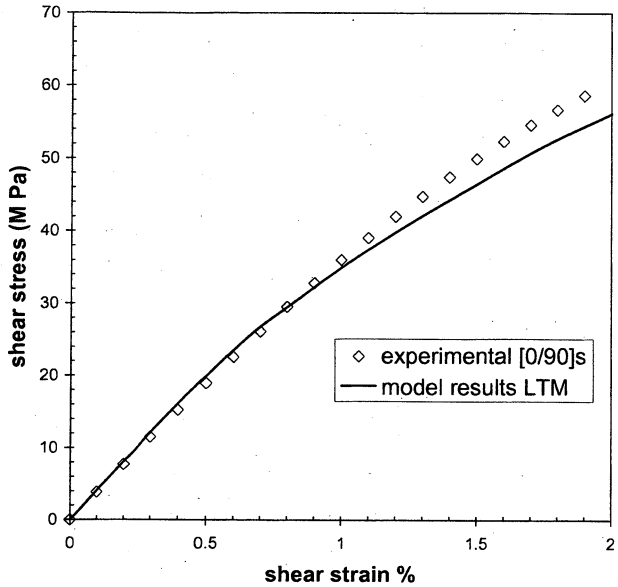

Fig. 6. Comparison of model prediction and experimental data for shear of [0/90]s laminate, LTM45EL-SM.

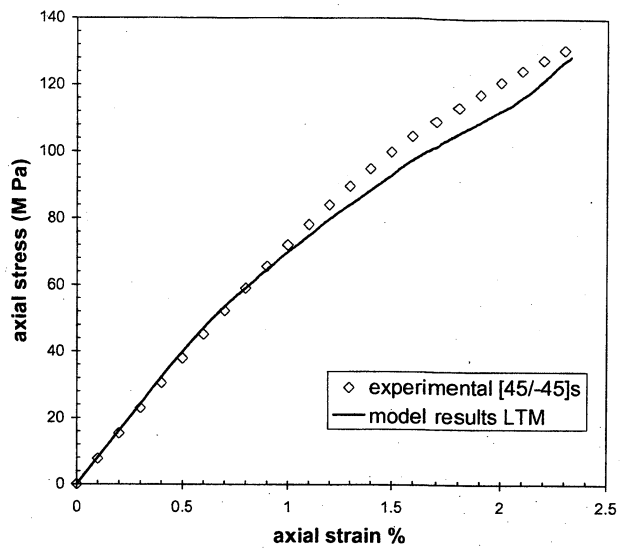

Fig. 7. Comparison of model prediction and experimental data for axial loading of [45/–45]s laminate, LTM45EL-SM.

Next, for T300/5208, comparison of predicted and experimental results for an inplane shear test of [0/90]2s is shown in Fig. 8. Comparison of predicted and experimental results for an axial loading test of [45/–45]2s is shown in Fig. 9.

The damage model can be used to predict the stress in the fiber and the matrix, as shown in Fig. 10 for Fiberite M40/949 carbon/epoxy unidirectional composite. The material properties are available in [36].

8. Conclusions

The proposed model utilizes nine damage parameters, which need to be adjusted with experimental data. Only experimental data available in he literature is needed. No especial tests are required beyond those commonly performed to characterize polymer matrix composites. The orthotropic nature of damage in polymer matrix composites is accounted for. Stress, damage, and degraded stiffness of each constituent are predicted. Damage induces stress redistribution. The model accounts for stress redistribution among the constituents

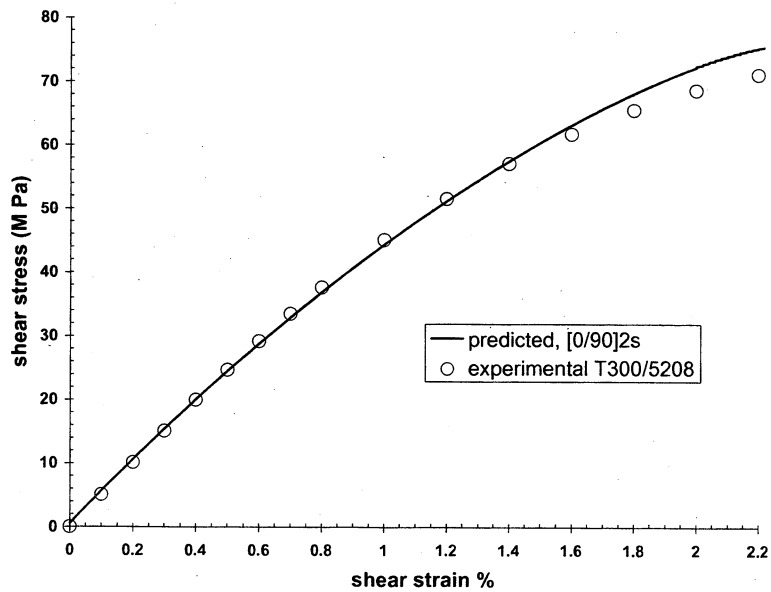

Fig. 8. Comparison of model prediction and experimental data for shear of [0/90]2s laminate, T300/5208.

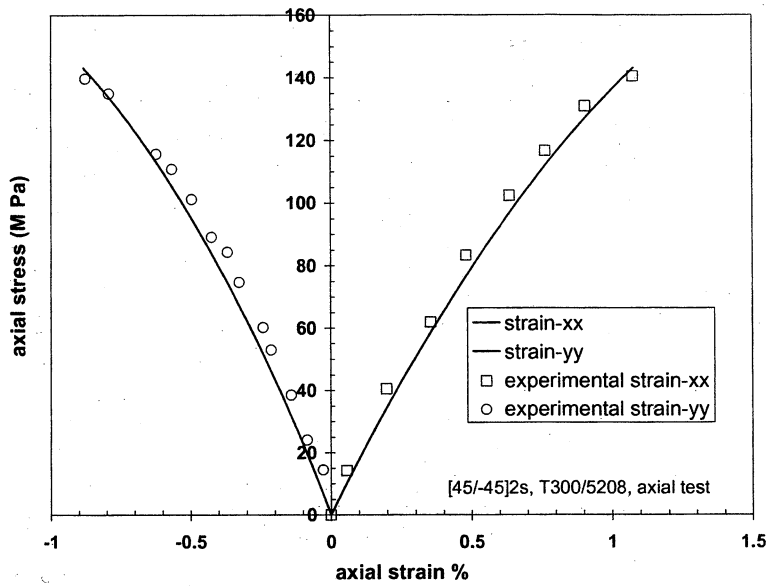

Fig. 9. Comparison of model prediction and experimental data for axial loading of [45/–45]2s laminate, T300/5208.

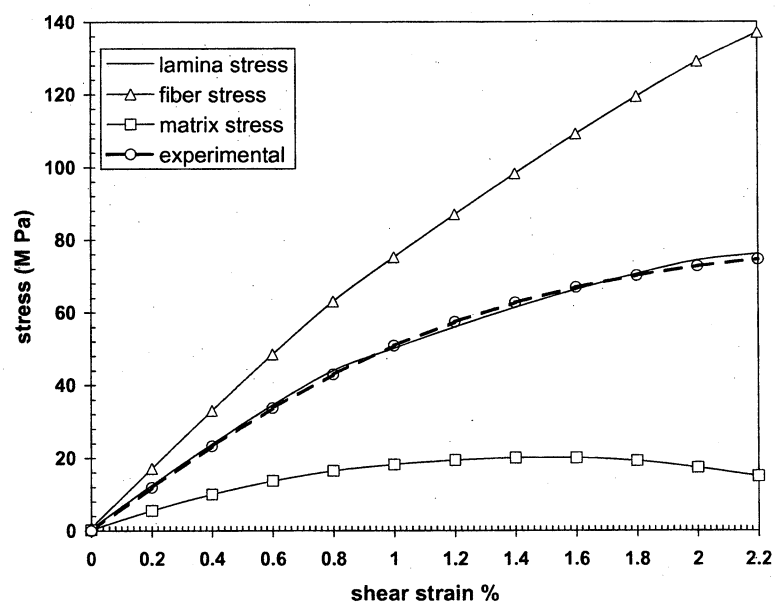

Fig. 10. Comparison of model prediction and experimental data for shear loading of Fiberite M40/949 unidirectional composite.

and among the laminae. Implementation of the model into Abaqus allows for analysis of complex structures but its current implementation is computationally expensive. Further work is envisioned to reduce the computational expense.

Acknowledgements

The financial support of the Federal Railroad Administration through grant #DT-FR-53-94-G-00039 is gratefully acknowledged.

References

[1] Abaqus user manual, Version 6.1, HKS, Pawtucket, RI.
[2] Abdelal GA. Three-phase constitutive model formicrobrittle fatigue damage of composites. Dissertation. West Virginia University, 2000.
[3] ASTM standards. High modulus fibers and composites, v15.03, 2000.
[4] Barbero EJ, Lonetti P. A damage model for composites defined in terms of available data. J Mech Compos Mater Struct 2001;8(4):299–316.
[5] Barbero EJ, DeVivo L. A constitutive model for elastic damage in fiber-reinforced PMC laminae. J Damage Mech 2001;10(1):73–93.

[6] Barbero EJ, Lonetti P. An inelastic damage model for fiber reinforced laminates. J Compos Mater 2002;36(8):941–62.
[7] Barbero EJ, Wen E. Compressive strength of production parts without compression testing. In: Composite structures: theory and practice, ASTM STP 1383. PA: ASTM; 2000.
[8] Barbero EJ. Introduction to composite materials design. Philadelphia, PA: Taylor & Francis; 1999.
[9] Barbero EJ. Prediction of compression strength of unidirectional polymer matrix composites. J Compos Mater 1998;32(5):483–502.
[10] Barbero EJ, Tomblin J. A damage mechanics model for compression strength of composites. Int J Solids Struct 1996;33(29):4379–93.
[11] Caceres A. Local damage analysis of fiber reinforced polymer matrix composites. Dissertation. Mechanical and Aerospace Engineering, West Virginia University, 1998.
[12] Cordebois JL, Sirodoff F. Damage induced elastic anisotropy. Colloque Euromech 115, Villard de Lans, France, 1979.
[13] Haberle JG. Strength and failure mechanisms of unidirectional carbon fibre-reinforced plastics under axial compression. PhD thesis. Imperial College, London, UK, 1991.
[14] Herakovich CT. Mechanics of fibrous composites. NY: John Wiley; 1998.
[15] Huang ZM. A unified micromechanical model for the mechanical properties of two constituent composite materials. Part I: elastic behavior. J Thermoplast Compos Mater 2000;13(July).
[16] Jamison RD, Schulte K, Reifsnider KL, Stinchcomb WW. Characterization and analysis of damage mechanisms in tension–tension fatigue of graphite/epoxy laminates. In: Effects of defects in composite materials, ASTM STP 836. American Society for Testing and Materials; 1984. p. 21–5.
[17] Janson J, Hult J. Damage mechanics and fracture mechanics: a combined approach. J Mec Appl 1977;1:69–84.
[18] Kasai Y, Saito M. Weibull analysis of strengths of various reinforcing filaments. Fibre Sci Technol 1979;12:21–9.
[19] Kelly K, Barbero EJ. The effect of fiber damage on longitudinal creep of a CFMMC. Int J Solids Struct 1993;30:3417–29.
[20] Krajcinovic D. Damage mechanics. Amsterdam: North Holland; 1996.
[21] Ladeveze P, LeDantec E. Damage modeling of the elementary ply for laminated composites. Compos Sci Technol 1992;43:257–67.
[22] Lonetti P, Barbero EJ, Zinno R, Greco F. Interlaminar damage model for polymer matrix composites. J Compos Mater 2003;37(16):1485–504.
[23] Luciano R, Barbero EJ. Formulas for the stiffness of composites with periodic microstructure. Int J Solids Struct 1995;31(21):2933–44.
[24] McDonough WG, Clough RB. The measurement of fiber strength parameters in fragmentation tests by using acoustic emissions. Compos Sci Technol 1996;56:119–1127.
[25] O'Brien TK. Stacking sequence effect on local delamination onset in fatigue. In: Proceedings of the International Conference on Advanced Composite Materials, February 15–19. Warrendale, PA, USA: Minerals, Metals and Materials Society (TMS); 1993. p. 399–406.
[26] Piggott MR, Liu K, Wang J. New experiments suggest that all the shear and some tensile failure processes are inappropriate subjects for ASTM standards. ASTM STP composite structures: theory and practice, 2000.
[27] Ramani VR, Williams PL. Axial fatigue of $[0/\pm 30]_{6S}$ graphite/epoxy. Ames Research Center, NASA, 1979.
[28] Razvan A, Bakis CE, Reifsnider KL. SEM investigation of fiber fracture in composite laminates. Mater Charact 1990;24(2):179–90.
[29] Rosen BW. The tensile failure of fibrous composites. AIAA J 1964;2(11):1985–91.
[30] Salpekar SA, O'Brien TK. Analysis of matrix cracking and local delamination in $(0/\theta/-\theta)$s graphite epoxy laminates under tensile load. J Compos Technol Res 1993;15(2):95–100.
[31] Schultheiz CR, McDonough WG, Shrikant K, Shutte CL, Mcturk KS, McAulife M, et al. In: 13th Symposium on Composites Testing and Design. PA: ASTM. 2001, p. 257–86.
[32] Voyiadjis GZ, Park T. Anisotropic damage of fiber-reinforced MMC using overall damage analysis. J Eng Mech 1995;121(11):1209–17.
[33] Voyiadjis GZ, Park T. Local and interfacial damage analysis of metal matrix composites. Int J Eng Sci 1995;33(11):1595–621.
[34] Voyiadjis GZ, Venson AR. Experimental damage investigation of a SiC–Ti aluminide metal matrix composite. Int J Solids Struct 1995;4:338–61.
[35] Voyiadjis GZ, Deliktas B. A coupled anisotropic damage model for the inelastic response of composite materials. Comput Meth Appl Mech Eng 2000;183:159–99.
[36] Wen E. Compressive strength prediction for composite unmanned aerial vehicles. Thesis. West Virginia University, Morgantown, WV, 1999.
[37] Yurgartis SW, Sternstein SS. Experiments to reveal the role of matrix properties and composite microstructure in longitudinal compression response of composite structures, ASTM, November 16– 17, 1992.
[38] Dragon TL, Hipp PA. Materials characterization and joint testing on the X-34 RLV. SAMPE J 1998;34(5):14–5.